Ultrasensitive Seawater pH Measurement by Capacitive Readout of Potentiometric Sensors

Kraikaew, Pitchnaree; Jeanneret Grosjean, Stéphane; Soda, Yoshiki; Cherubini, Thomas John; Bakker, Eric

How to cite

KRAIKAEW, Pitchnaree et al. Ultrasensitive Seawater pH Measurement by Capacitive Readout of Potentiometric Sensors. In: ACS Sensors, 2020, vol. 5, n° 3, p. 650–654. doi: 10.1021/acssensors.0c00031

This publication URL: https://archive-ouverte.unige.ch/unige:141065
Publication DOI: 10.1021/acssensors.0c00031

ACS SENSORS

pubs.acs.org/acssensors

Letter

Ultrasensitive Seawater pH Measurement by Capacitive Readout of Potentiometric Sensors

Pitchnaree Kraikaew, Stéphane Jeanneret, Yoshiki Soda, Thomas Cherubini, and Eric Bakker*

Cite This: *ACS Sens.* 2020, 5, 650–654

Read Online

ACCESS | Metrics & More | Article Recommendations | Supporting Information

ABSTRACT: Potentiometric pH probes remain the gold standard for the detection of pH but are not sufficiently sensitive to reliably detect ocean acidification at adequate frequency. Here, potentiometric probes are made dramatically more sensitive by placing a capacitive electronic component in series to the pH probe while imposing a constant potential over the measurement circuit. Each sample change now triggers a capacitive current transient that is easily identified between the two equilibrium states, and is integrated to reveal the accumulated charge. This affords dramatically higher precision than with traditional potentiometric probes. pH changes down to 0.001 pH units are easily distinguished in buffer and seawater samples, at a precision (standard deviation) of 28 μpH and 67 μpH, respectively, orders of magnitude better than what is possible with potentiometric pH probes.

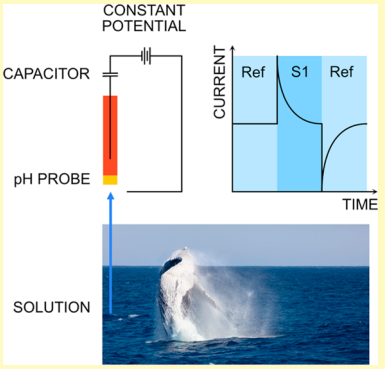

KEYWORDS: *capacitive readout, small pH change, seawater, ocean acidification, pH electrode, ionophore*

The measurement of pH is of enormous importance in most chemical, biological, and environmental processes.[1−4] Atmospheric carbon dioxide (CO_2) output from anthropogenic sources including fossil fuel combustion and deforestation results in its gradual absorption by marine systems. This oceanic uptake serves to moderate atmospheric CO_2 but causes a reduction of surface ocean pH.[5] This significantly alters the chemical balance of the marine carbonate system, with a potentially dramatic impact to marine biota and ocean ecosystems.[6,7] To accurately understand how ocean acidification impacts marine life, it is necessary to quantify seawater pH variability at an adequate measurement frequency.

While they remain the gold standard, the precision of potentiometric pH probes is limited because potential drifts/uncertainties (up to 0.02 pH units per day) may become difficult to distinguish from the desired change in pH.[8,9] Potentiometric seawater pH measurements have been found to exhibit a precision of about 0.003 pH units,[10] or about 0.2 mV. Ion-selective field-effect transistors (ISFET), on the other hand, gave a precision better than 0.0005 pH units over hours and 0.005 over weeks for the same application.[11,12] Similar to a conventional glass electrode, ISFETs are still required regular calibration using standard pH buffer.[13] Spectrophotometry by indicator dye solution affords improved precision, giving a variability of just 0.4 mpH units for seawater.[14,15] For this, the indicator solution must be adequately stored to ensure long-term stability,[16] and the indicator needs to be highly purified to reduce errors in the pH calculated from absorbance data.[17,18] However, spectrophotometric pH is not the same as pH reported by potentiometry, because very different assumptions are involved in the measurement. With pH indicator dyes, the activity coefficient of the dye depends on solution ionic strength and there is no liquid junction potential.

Here, the determination of pH at very high precision is achieved by modifying the electronic readout of electrochemical pH probes. Instead of observing potentials over time, which are difficult to distinguish from unrelated potential drifts, one allows a transient current to occur for a given pH change by placing an electronic capacitor component in series to the pH probe and holding the cell potential constant. The small current excursions can be easily identified, background-subtracted, and integrated to give a charge that serves as a sensor signal.

The approach proposed here builds on earlier work by the group of Bobacka[19,20] on the basis of a conducting polymer, poly(3,4-ethylenedioxythiophene) (PEDOT) doped with poly(styrenesulfonate) (PSS), that serves as a capacitive layer between electrode and ion-selective membrane. Vanamo et al. demonstrated that the measured current signal can be amplified by increasing the thickness, and therefore the redox capacitance, of the solid contact conducting polymer.[21]

Received: January 6, 2020
Accepted: February 28, 2020
Published: February 28, 2020

https://dx.doi.org/10.1021/acssensors.0c00031
ACS Sens. 2020, 5, 650–654

The theory for this transduction method suggests that an increasing capacitance, C, results in a larger measured charge, Q, as follows.[22]

$$Q = C\frac{s}{z_i}\log\left(\frac{a_i(\text{initial})}{a_i(\text{final})}\right) \quad (1)$$

where s is the Nernstian slope (59.2 mV at 25 °C), z_i is the charge of the detected ion (for hydrogen ions, z_i = 1), and a_i(initial) and a_i(final) are the activity of the detected ion i before and after the sample composition change.

Here, ultrasensitive pH measurements are achieved by using, for the first time, electronic capacitor components instead of conducting polymer layers. This likely provides better stability and further gives exquisite control for tuning the sensitivity of the method to the pH change of interest. Scheme 1 shows the capacitive readout principle with an ion-selective membrane element connected in series with an electronic capacitor. The initial open circuit potential (OCP) of the measurement cell is kept constant. A change in ion activity results in a potential change at the indicator electrode in agreement with the Nernst equation, which must be compensated by an opposite potential change of the capacitor. For measuring small pH changes, the compositional change must reach the indicator electrode abruptly to achieve well-resolved current transients that can be subtracted from the background. A segmented flow separates the sample solution from a reference solution with an air gap[23−25] to minimize dispersion. Each measurement involves a sequential alternation of sample (S1) and reference solution (Ref), giving a sharp transition that reflects the ion activity change (see top right in Scheme 1).

Scheme 1. Potential Change Observed at a pH Electrode Is Compensated over a Capacitive Element Placed in Series as the Overall Cell Potential Is Held Constant[a]

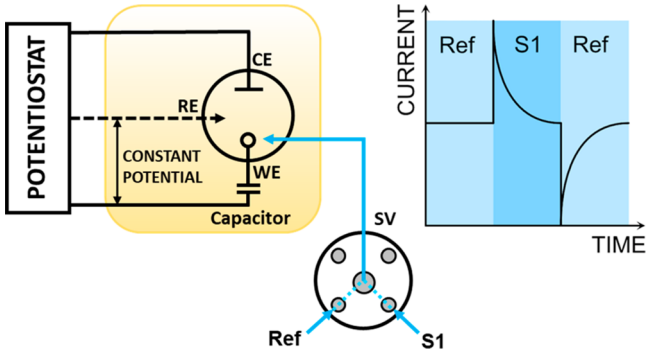

[a]The alternating introduction of a reference (Ref) and sample solution (S1) by a switch valve (SV) results in current transients that are easily identified and quantified to make ultrasensitive pH measurements possible. The important application for this advance is the monitoring of ocean acidification at high time resolution.

Potentiometric probes consisting of an Ag/AgCl sensing element served as an initial model system because their potential is resistant to the passage of current. The detection protocol involves the measurement of the open circuit potential (OCP) in the reference solution, which is then imposed at the same amplitude over the course of the experiment. When a sample of different concentration reaches the electrode, a transient current spike is observed (Figure 1A). Decreasing sample concentrations result in a reversible change in the opposite direction. Integration of the transient currents provide the corresponding cumulated charge over time (Figure 1B).

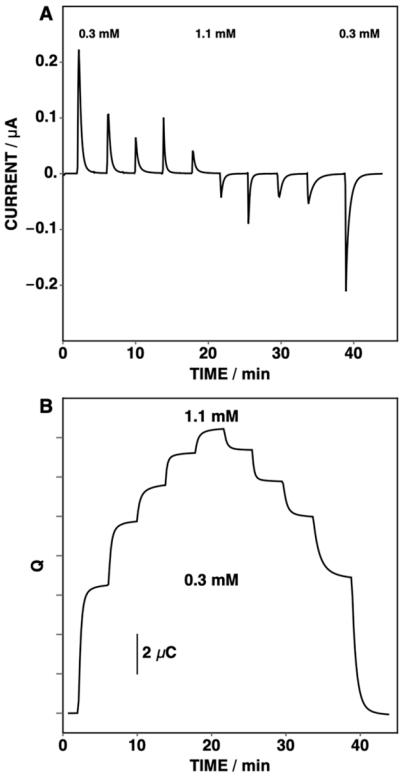

Figure 1. (A) Observed current transients and (B) integrated charge upon increasing the chloride concentration from 0.1 mM to 1.1 mM in 0.2 mM steps, and back to 0.1 mM, using the chloride sensitive Ag/AgCl electrode as initial model system to demonstrate the principle.

A range of commercially available capacitors (4.7 to 470 μF) was evaluated. As shown in Figure 2A, a linear dependence of accumulated charge on the logarithmic chloride activity is obtained with the Ag/AgCl electrode in agreement with eq 1 and using the known capacitance of the electronic element (solid lines are predicted from nominal capacitances). Figure 2A,B shows that the observed slopes for charge Q vs log a_{Cl^-} agree well with those predicted from eq 1 for a wide range of capacitances. Larger capacitances result in a greater charge, proportional to Csz_i^{-1} in eq 1, which can therefore be amplified for better sensitivity. An excessive charge passing through the cell should be avoided to minimize sample and membrane perturbations. For this reason, larger capacitances are best suited for small sample concentration changes to limit the resulting charge.

The constant-potential coulometric approach integrated into an automated air-segmented flow system was applied to demonstrate the reversible detection of pH change using an H^+-selective electrode. The high resistance of commercial glass pH probes (50 to 500 MΩ) make it too difficult to pass appreciable charge and should result in RC time constants on the order of hours. The membranes used here were polymeric membrane electrodes containing tridodecylamine as lipophilic H^+-ionophore that are suitable for measurements over periods of weeks (see Supporting Information and Figure S1). The membrane electrode chosen here is of the aqueous inner solution type, and future work will evaluate whether the approach may be applicable with solid-contact membrane

https://dx.doi.org/10.1021/acssensors.0c00031
ACS Sens. 2020, 5, 650−654

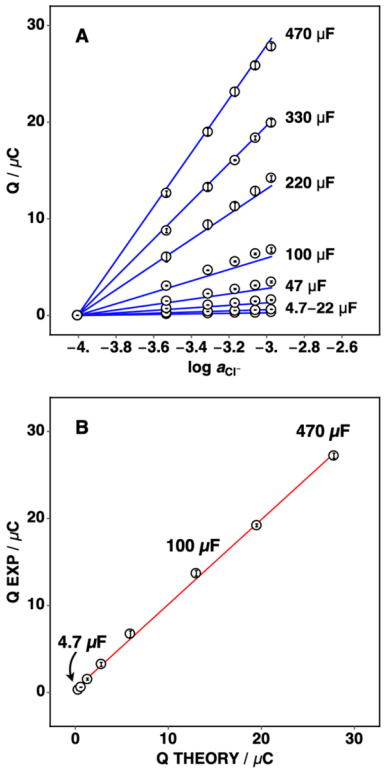

Figure 2. (A) Calibration curves for integrated charge vs logarithmic chloride activity for the indicated capacitances, using an Ag/AgCl sensing element as model system. Blue lines are theoretical based on eq 1. (B) Correspondence between theoretical (eq 1) and observed charge upon a 10-fold activity change in the sample for the same range of capacitances (4.7 μF to 470 μF).

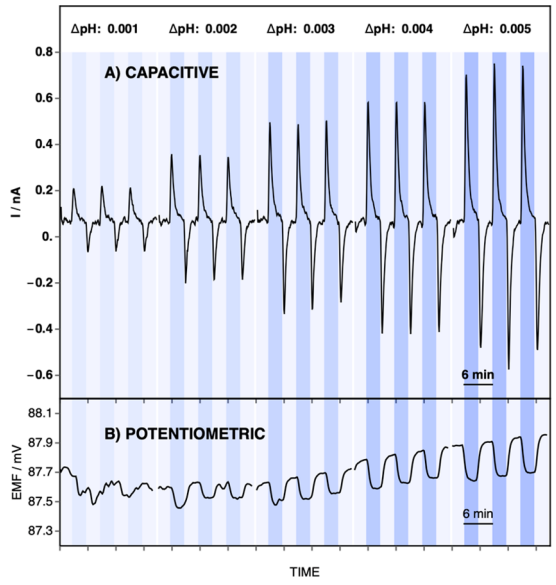

Figure 3. (A) Measurement of small pH change in the range of 0.001 to 0.005 units with a 100 μF capacitance. Detection of the reference sample (light background color) is followed by the sample of increasing pH (darker background), repeated three times for each pH value (constant flow rate of 333 μL min^{-1}). Negative current transients indicate return to reference solution of lower pH. (B) Same measurement as for (A), but using zero current potentiometry as readout in the absence of capacitive element.

electrodes. Small, well-defined changes of pH were achieved by automatic titration, delivering precise volumes of NaOH into a 0.1 M Tris buffer. Figure 3 illustrates the observed reversible transient current spikes over time for pH changes that range from 0.001 to 0.005 pH units relative to the reference solution, using a 100 μF capacitor for improved sensitivity. The measurement of reference solution−sample−reference solution gives two current transients, one positive and one negative. The first peak is used as the signal, while the reversal peak serves to establish the new current baseline for subsequent measurements. The transients are found to be sufficiently sharp (see Figure 3A). Linear regression of charge and ΔpH is shown in Figure 4A, described by$Q = 1.37 \times 10^{-9}C + 56.7 \times 10^{-7}C \times \Delta\text{pH}$ and r^2 of 0.9993. Equation 1 may be rewritten to represent pH change instead of ion activity as follows:

$$Q = Cs\Delta\text{pH} \quad (2)$$

where s is electrode slope (ideally 58.6 mV at 22 °C) and C is the capacitance used. For the data in Figure 3A, s is near-Nernstian at 56.7 mV (see calibration curve in Figure 4A) and in good agreement with eq 2. The observed reproducibility (average standard deviations, shown as error bars in Figure 4A) is found as 28 × 10^{-6} pH units, which in potentiometry would correspond to a potential change of a mere 1.7 μV.

The proposed method was compared with zero current potentiometry using the same pH electrode (without capacitor) in otherwise the same measurement setup, sequentially comparing each sample to the reference solution. The corresponding EMF vs time traces are shown in Figure 3B. For the smallest pH changes, it becomes difficult to distinguish the individual potential responses, while for larger ones, the differences become evident, but so is the influence of potential drift on the pH data. Figure S2 shows the corresponding plot of measured EMF change vs ΔpH, with the slope (sensitivity) indicated as a solid line (ΔEMF = −0.04 mV − 37.0 mV × ΔpH and r^2 = 0.98), which is significantly sub-Nernstian, which contrasts to the expected behavior over a wide pH range (Figure S3). The average standard deviation is found as 0.012 mV or 1.4 mpH units, which is about 2 orders of magnitude worse than with the approach introduced here. The systematic error originating in the deviation from the Nernstian response slope further exacerbates this uncertainty. Based on the data presented here, the capacitive readout allows one to achieve ultraprecise pH readings that significantly surpass that of potentiometry for the determination of pH.

Fluctuations in seawater pH are mainly driven by an increase in atmospheric CO_2, shifting the carbonate buffer system and adversely impacting the development of marine species, particularly calcifying organisms. Since the industrial revolution, the average ocean surface pH has decreased by 0.1 pH units[26] at a current rate of 0.002 pH units per year.[27,28] Capturing pH variations at a detection frequency in the order of days is important to assess ocean acidification dynamics. The precision of potentiometric pH probes is not adequate for this task.

The proposed method is demonstrated to measure ultrasmall pH changes of seawater that was sourced from Arcachon Bay near Bordeaux in Southwestern France. To eliminate potential sources of error from CO_2 re-equilibration with the atmosphere, which could not be avoided with the current cell design (see Figure S4), the seawater samples were treated with Tris buffer to stabilize their pH values. The total pH scale was used where sulfate ion is also considered by titration to identify

https://dx.doi.org/10.1021/acssensors.0c00031
ACS Sens. 2020, 5, 650−654

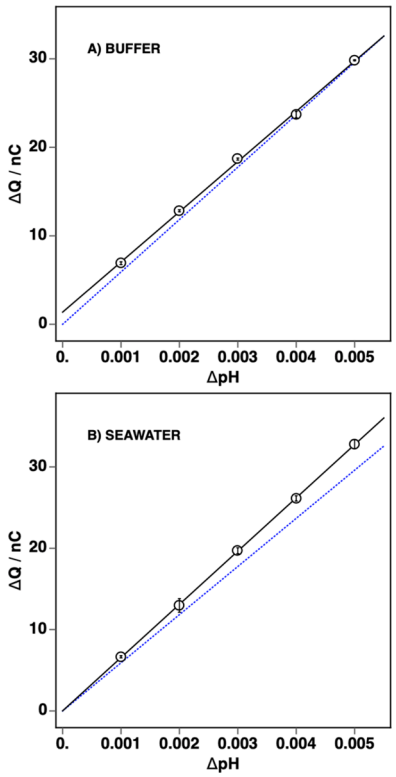

Figure 4. (A) Calibration curve of integrated charge from the current transients shown in Figure 3A as a function of pH change. Error bars are standard deviations (n = 3), corresponding to an average of 28 μpH units. (B) Calibration curve from the same type of experiment as in (A), but with seawater sample from Arcachon Bay (average standard deviation of 67 μpH). Blue dashed lines are theoretical based on eq 1 and deviate slightly more for seawater, likely given by the limited extrapolation precision to find the pH change. The seawater sample pH was stabilized to minimize systematic errors (see text).

the pK_a value (Figure S5). Figure 4B shows the observed integrated charge as a function of pH for seawater under otherwise the same experimental conditions as for Figure 4A. Regression analysis gives $Q = 0.01 \times 10^{-9}C + 65.5 \times 10^{-7}C \times \Delta$pH ($r^2$ = 0.9999) corresponding to a near-Nernstian slope of 65.5 mV with the 100 μF capacitive elements used here (eq 2). The reproducibility calculated as the average of the standard deviations is 67 μpH, which compares well to the data in Figure 4A. The same samples assessed potentiometrically (Figure S4) give potential traces that are too difficult to distinguish reliably. While the observed EMF visibly drifts, the ΔEMF versus ΔpH curve plotted as a function of time in Figure S4 (inset) gives a calculated standard deviation of 0.7 mpH or 0.017 mV. Given the sub-Nernstian response slope for this data, the actual error is expected to be larger.

Direct potentiometry has been in use for over a century for the determination of pH. While it remains the gold standard, it does not provide the precision required to assess very small pH changes in important applications such as ocean acidification. We have shown here that potentiometric pH probes can be made orders of magnitude more sensitive by imposing the potential change at the pH electrode over an electronic capacitive element placed in series while maintaining a constant cell potential. The resulting current transient required to charge the capacitor with the same potential amplitude (of opposite sign) is much easier to identify and isolate than a potential−time trace. The precision of this technique is found to be extraordinary, corresponding to just a few microvolts or dozens of micro-pH units and may serve as a basis for applications where very small concentration changes need to be reliably quantified, as in ocean acidification. We note that this advance concerns the underlying measurement principle only. Care must be taken to avoid systematic errors originating from sample manipulation steps, especially re-equilibration with atmospheric CO_2.

■ ASSOCIATED CONTENT

Supporting Information

The Supporting Information is available free of charge at https://pubs.acs.org/doi/10.1021/acssensors.0c00031.

Experimental section, instrumentation and measurements, sample preparation, preparation of the electrodes, in-line measurement, schematic illustration of automated flow system, potentiometric measurement of small pH change for Tris buffer and seawater sample, and other data (PDF)

■ AUTHOR INFORMATION

Corresponding Author

Eric Bakker − *Department of Inorganic and Analytical Chemistry, University of Geneva CH-1211 Geneva, Switzerland;* orcid.org/0000-0001-8970-4343; Email: Eric.Bakker@unige.ch

Authors

Pitchnaree Kraikaew − *Department of Inorganic and Analytical Chemistry, University of Geneva CH-1211 Geneva, Switzerland*

Stéphane Jeanneret − *Department of Inorganic and Analytical Chemistry, University of Geneva CH-1211 Geneva, Switzerland*

Yoshiki Soda − *Department of Inorganic and Analytical Chemistry, University of Geneva CH-1211 Geneva, Switzerland*

Thomas Cherubini − *Department of Inorganic and Analytical Chemistry, University of Geneva CH-1211 Geneva, Switzerland*

Complete contact information is available at: https://pubs.acs.org/10.1021/acssensors.0c00031

Author Contributions

P.K., Y.S., and E.B. conceived the idea and designed the experiments. S.J. and T.C. carried out the device fabrication and created software. P.K. and E.B. analyzed the data and wrote the paper.

Notes

The authors declare no competing financial interest.

■ ACKNOWLEDGMENTS

This research was partially supported by Swiss National Science Foundation (SNSF). P.K. thanks the Development and Promotion of Science and Technology Talents Project (DPST) of Thailand for financial support. The seawater sample was kindly provided by Marylou Tercier -Waeber, University of Geneva.

https://dx.doi.org/10.1021/acssensors.0c00031
ACS Sens. 2020, 5, 650−654

REFERENCES

(1) Wang, X.-d.; Meier, R. J.; Wolfbeis, O. S. Fluorescent pH-Sensitive Nanoparticles in an Agarose Matrix for Imaging of Bacterial Growth and Metabolism. *Angew. Chem., Int. Ed.* **2013**, *52*, 406−409.

(2) Kim, J.; Campbell, A. S.; de Ávila, B. E.-F.; Wang, J. Wearable biosensors for healthcare monitoring. *Nat. Biotechnol.* **2019**, *37*, 389−406.

(3) Nakata, S.; Shiomi, M.; Fujita, Y.; Arie, T.; Akita, S.; Takei, K. A wearable pH sensor with high sensitivity based on a flexible charge-coupled device. *Nat. Electron.* **2018**, *1*, 596−603.

(4) Anes, B.; Bettencourt da Silva, R. J. N.; Oliveira, C.; Camões, M. F. Seawater pH measurements with a combination glass electrode and high ionic strength TRIS-TRIS HCl reference buffers − An uncertainty evaluation approach. *Talanta* **2019**, *193*, 118−122.

(5) Caldeira, K.; Wickett, M. E. Anthropogenic carbon and ocean pH. *Nature* **2003**, *425*, 365−365.

(6) Orr, J. C.; Fabry, V. J.; Aumont, O.; Bopp, L.; Doney, S. C.; Feely, R. A.; Gnanadesikan, A.; Gruber, N.; Ishida, A.; Joos, F.; Key, R. M.; Lindsay, K.; Maier-Reimer, E.; Matear, R.; Monfray, P.; Mouchet, A.; Najjar, R. G.; Plattner, G.-K.; Rodgers, K. B.; Sabine, C. L.; Sarmiento, J. L.; Schlitzer, R.; Slater, R. D.; Totterdell, I. J.; Weirig, M.-F.; Yamanaka, Y.; Yool, A. Anthropogenic ocean acidification over the twenty-first century and its impact on calcifying organisms. *Nature* **2005**, *437*, 681−686.

(7) Doney, S. C.; Fabry, V. J.; Feely, R. A.; Kleypas, J. A. Ocean Acidification: The Other CO2 Problem. *Annu. Rev. Mar. Sci.* **2009**, *1*, 169−192.

(8) Seiter, J. C.; DeGrandpre, M. D. Redundant chemical sensors for calibration-impossible applications. *Talanta* **2001**, *54* (1), 99−106.

(9) Dickson, A. G. The measurement of sea water pH. *Mar. Chem.* **1993**, *44* (2), 131−142.

(10) Fuhrmann, R.; Zirino, A. High-resolution determination of the pH of seawater with a flow-through system. *Deep-Sea Res., Part A* **1988**, *35*, 197−208.

(11) Martz, T. R.; Connery, J. G.; Johnson, K. S. Testing the Honeywell Durafet® for seawater pH applications. *Limnol. Oceanogr.: Methods* **2010**, *8* (5), 172−184.

(12) Johnson, K. S.; Jannasch, H. W.; Coletti, L. J.; Elrod, V. A.; Martz, T. R.; Takeshita, Y.; Carlson, R. J.; Connery, J. G. Deep-Sea DuraFET: A Pressure Tolerant pH Sensor Designed for Global Sensor Networks. *Anal. Chem.* **2016**, *88*, 3249−3256.

(13) Bresnahan, P. J.; Martz, T. R.; Takeshita, Y.; Johnson, K. S.; LaShomb, M. Best practices for autonomous measurement of seawater pH with the Honeywell Durafet. *Methods Oceanogr* **2014**, *9*, 44−60.

(14) Clayton, T. D.; Byrne, R. H. Spectrophotometric seawater pH measurements: total hydrogen ion concentration scale calibration of m-cresol purple and at-sea results. *Deep Sea Res., Part I* **1993**, *40*, 2115−2129.

(15) Carter, B. R.; Radich, J. A.; Doyle, H. L.; Dickson, A. G. An automated system for spectrophotometric seawater pH measurements. *Limnol. Oceanogr.: Methods* **2013**, *11*, 16−27.

(16) DeGrandpre, M. D.; Hammar, T. R.; Smith, S. P.; Sayles, F. L. In situ measurements of seawater pCO2. *Limnol. Oceanogr.* **1995**, *40*, 969−975.

(17) Yao, W.; Liu, X.; Byrne, R. H. Impurities in indicators used for spectrophotometric seawater pH measurements: Assessment and remedies. *Mar. Chem.* **2007**, *107*, 167−172.

(18) Liu, X.; Patsavas, M. C.; Byrne, R. H. Purification and Characterization of meta-Cresol Purple for Spectrophotometric Seawater pH Measurements. *Environ. Sci. Technol.* **2011**, *45*, 4862−4868.

(19) Hupa, E.; Vanamo, U.; Bobacka, J. Novel Ion-to-Electron Transduction Principle for Solid-Contact ISEs. *Electroanalysis* **2015**, *27*, 591−594.

(20) Han, T.; Mattinen, U.; Bobacka, J. Improving the Sensitivity of Solid-Contact Ion-Selective Electrodes by Using Coulometric Signal Transduction. *ACS Sensors* **2019**, *4*, 900−906.

(21) Vanamo, U.; Hupa, E.; Yrjänä, V.; Bobacka, J. New Signal Readout Principle for Solid-Contact Ion-Selective Electrodes. *Anal. Chem.* **2016**, *88*, 4369−4374.

(22) Jarolímová, Z.; Han, T.; Mattinen, U.; Bobacka, J.; Bakker, E. Capacitive Model for Coulometric Readout of Ion-Selective Electrodes. *Anal. Chem.* **2018**, *90*, 8700−8707.

(23) Alexander, P. W.; Seegopaul, P. Rapid-flow continuous analysis with ion-selective electrodes. *Anal. Chem.* **1980**, *52*, 2403−2406.

(24) Hibbert, D. B.; Alexander, P. W.; Rachmawati, S.; Caruana, S. A. Multiple sensor response in segmented flow analysis with ion-selective electrodes. *Anal. Chem.* **1990**, *62*, 1015−1019.

(25) Borges, E. P.; Martelli, P. B.; Reis, B. F. Automatic Stepwise Potentiometric Titration in a Monosegmented Flow System. *Microchim. Acta* **2000**, *135*, 179−184.

(26) Caldeira, K.; Wickett, M. E. Ocean model predictions of chemistry changes from carbon dioxide emissions to the atmosphere and ocean. *J. Geophys. Res.* **2005**, *110*, 110.

(27) Dore, J. E.; Lukas, R.; Sadler, D. W.; Church, M. J.; Karl, D. M. Physical and biogeochemical modulation of ocean acidification in the central North Pacific. *Proc. Natl. Acad. Sci. U. S. A.* **2009**, *106*, 12235.

(28) Byrne, R. H.; Mecking, S.; Feely, R. A.; Liu, X. Direct observations of basin-wide acidification of the North Pacific Ocean. *Geophys. Res. Lett.* **2010**, *37*, 1 DOI: 10.1029/2009GL040999.

https://dx.doi.org/10.1021/acssensors.0c00031
ACS Sens. 2020, 5, 650−654